ELSEVIER

Journal of Nuclear Materials 299 (2001) 68–76

journal of nuclear materials

www.elsevier.com/locate/jnucmat

Effect of ensemble of stress concentrators on the ultimate tensile strength of material

Roman E. Voskoboinikov *

Russian Scientific Center, Kurchatov Institute, Kurchatov Square 1, Moscow 123182, Russia

Received 20 April 2001; accepted 23 July 2001

Abstract

Equilibrium of a (quasi)brittle crack in a uniaxially loaded material with an infinite linear row of stress concentrators is investigated. Dependence of the equilibrium crack length on the applied stress, internal loading, stress concentrator size, distance between neighboring concentrators etc. is found. Evaluation of the ultimate tensile strength of material with the linear row of voids, gas bubbles and secondary phase precipitates was carried out. © 2001 Elsevier Science B.V. All rights reserved.

PACS: 62.20.Mk; 81.40.Np; 81.40.Cd; 46.30.N

1. Introduction

Fracture of many structural materials occurs through crack nucleation and growth. The theory of crack behavior in mono-phase homogeneous materials has been developed in detail but the results obtained are of limited relevance for description of fracture of advanced structural materials with complicated multi-phase composition. Secondary phase precipitates, gas bubbles, voids and their ensembles are common features of microstructure of modern structural materials. These inhomogenities behave as stress concentrators. They can significantly modify the stress field near the crack and noticeably affect its nucleation and growth.

A number of studies have been carried out in order to investigate crack equilibrium in stress fields modified by stress concentrators, see e.g., [1–7]. The results published in [1–6] were obtained for a solitary stress concentrator and can be used only in the case of a dilute ensemble of stress concentrators. However, sometimes ordered configurations of stress concentrators are formed. Provided the distance between neighboring concentrators is of the order of (or less than) their size, the collective behavior of stress concentrators should be taken into consideration. An example of such behavior for an infinite row of gas filled cracks was investigated in [7]. However, it is of interest to study the collective behavior of stress concentrators of other shapes.

In the present paper crack equilibrium in the uniaxially loaded material with an infinite linear row of circular stress concentrators is investigated. Dependence of equilibrium crack length on the applied stress, internal loading, stress concentrator size and type and the distance between concentrators is evaluated. Reduction of the ultimate tensile strength by linear arrays of voids, gas bubbles and/or secondary phase precipitates is demonstrated.

2. Problem set

Nucleation and equilibrium of a wedge crack in strained multi-phase material is investigated in terms of two-dimensional geometry (plain strain). Though in general both the loading geometry and the shape of stress concentrators are usually three-dimensional, the simplification proposed here allows the qualitative behavior of cracks formed at stress concentrators to be elucidated. Moreover, in certain cases the results

* Tel.: +7-095 196 9766; fax: +7-095 196 4546.

E-mail address: roman@dni.polyn.kiae.su (R.E. Voskoboinikov).

0022-3115/01/$ - see front matter
PII: S 0 0 2 2 - 3 1 1 5 (0 1) 0 0 6 6 9 - 9

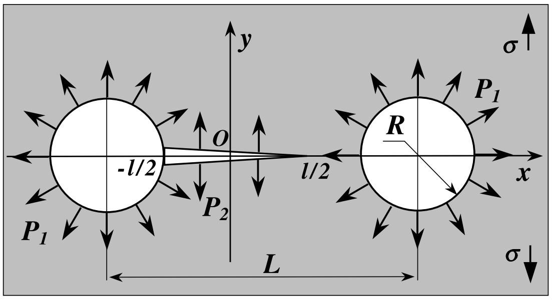

Fig. 1. Geometry of the problem.

obtained within two-dimensional consideration are directly applicable for description of the relevant phenomena, such as hydrogen embrittlement of zirconium based alloys or crack formation at a chain of secondary phase precipitates or gas bubbles at grain boundaries in steels [8,9] under irradiation.

Let us consider a material with an infinite linear row of circular stress concentrators of radius R. The centers of stress concentrators in the row lie on the x-axis of a Cartesian coordinate system. The distance between the centers of neighboring stress concentrators is L, $2R < L < \infty$. A (quasi)brittle crack of length l, $0 \leqslant l \leqslant L - 2R$ is formed on a stress concentrator in the row. The crack is treated here as a cut along the x-axis. The origin O of the coordinate system is chosen in the center of the crack. The material is loaded with uniaxial stress σ along the y-axis. The surfaces of stress concentrators and crack are loaded with normal stress P_1 and P_2, respectively (see Fig. 1). The stresses P_1 and P_2 are assumed to be positive provided they are directed out of a concentrator or the crack.

3. Governing equations

Mechanical stability of a material with a crack of length l requires the force balance at the crack surface to be fulfilled:

$$\sigma_{ij}n_j\big|_S + P_i(x) = 0, \quad (i,j = x,y), \\ S : (-l/2 \leqslant x \leqslant l/2, y = 0), \tag{1}$$

where $\mathbf{n}$ is a unit vector of the outward normal to the crack surface S; $\mathbf{P}(x)$ is the total force acting at the crack surface. Absence of a shear stress resulting from the symmetry of the problem makes it possible to reduce Eq. (1) to the following form:

$$\sigma_{yy}(x) = -P(x),$$

where $P(x)$ is the component of the total force $\mathbf{P}(x)$ normal to the crack surface. In our case $P(x)$ can be written as

$$P(x) = -P_2 - \sigma_{\theta\theta}(x) + S(h(x)). \tag{2}$$

Here $S(x)$ is the adhesive force acting at the crack tip of length d, $a \ll d \ll L$, where a is the interatomic distance [10]. Stress $\sigma_{\theta\theta}(x)$ is acting in the plain $y = 0$ in the loaded material without crack. The first two terms of the expansion of stress $\sigma_{\theta\theta}(x)|_{y=0}$ into series over $(R/L)^2$ is given by [11]

$$\sigma_{\theta\theta}(x) = \sigma^{(0)}_{\theta\theta}(x) + \sigma^{(1)}_{\theta\theta}(x)\frac{R^2}{L^2}, \tag{3}$$

where

$$\sigma^{(0)}_{\theta\theta}(x) = \frac{\sigma}{2}\left[2 + \left(1 + \frac{2P_1}{\sigma}\right)\left(\frac{R}{Q(x)}\right)^2 + 3\left(\frac{R}{Q(x)}\right)^4\right]$$

and

$$\sigma^{(1)}_{\theta\theta}(x) = \frac{\pi^2\sigma}{6}\left(\left(1 + \frac{2P_1}{\sigma}\right) + 2\left(\frac{R}{Q(x)}\right)^2 \right. \\ \left. + 3\left(\frac{2P_1}{\sigma} - 1\right)\left(\frac{R}{Q(x)}\right)^4\right),$$

where

$$Q(x) = x + R + l/2 - nL, \quad n = 0, \pm1, \pm2, \pm3, \ldots \\ nL - (L/2 + R + l/2) \leqslant x \\ \leqslant (n+1)L - (L/2 + R + l/2). \tag{4}$$

The condition of mechanical stability of a crack in a strained material is given by the following equation (see e.g., [12]):

$$\int_{-l/2}^{l/2} \frac{\sigma_{yy}(x)\,\mathrm{d}x}{\sqrt{l^2 - 4x^2}} = 0. \tag{5}$$

4. The condition of mechanical stability

In order to describe the dependence of the equilibrium crack length on internal (size and type of stress concentrator, distance between neighboring concentrators etc.) and external (applied stress) parameters the following non-dimensional variables are defined:

$$\eta = \frac{2x}{l}, \quad \rho = \frac{2R}{l}, \quad \lambda = \frac{2L}{l}. \tag{6}$$

Substituting Eqs. (2), (3) and (6) into (5) and carrying out integration, the condition of mechanical stability is obtained in the following form:

$$-\frac{\sqrt{2}K}{\sqrt{l}} + \pi(\sigma + P_2) + \left(\frac{\sigma}{2} + P_1\right)I_2(\rho,\lambda) \\ + \frac{3\sigma}{2}I_4(\rho,\lambda) + \Omega(\rho,\lambda)\frac{\rho^2}{\lambda^2} = 0, \tag{7}$$

where K is the stress intensity factor [13], defined by

$$K = \int_0^\infty \frac{S(h(x))}{\sqrt{x}}\,\mathrm{d}x; \tag{8}$$

function $\Omega(\rho, \lambda)$ is given by

$$\Omega(\rho, \lambda) = \frac{\pi^2}{6}(\pi(\sigma + 2P_1) + 2\sigma I_2(\rho, \lambda) + 3(2P_1 - \sigma)I_4(\rho, \lambda)), \tag{9}$$

and functions $I_2(\rho, \lambda)$ and $I_4(\rho, \lambda)$ are equal to

$$I_2(\rho, \lambda) = \begin{cases} \int_{-1}^{1} \frac{\rho^2\,\mathrm{d}\eta}{(\rho+\eta+1)^2\sqrt{1-\eta^2}}, \\ \quad \frac{\lambda}{2} - (\rho + 1) \geqslant 1 \\ \int_{-1}^{\lambda/2-(\rho+1)} \frac{\rho^2\,\mathrm{d}\eta}{(\rho+\eta+1)^2\sqrt{1-\eta^2}} \\ \quad + \int_{\lambda/2-(\rho+1)}^{1} \frac{\rho^2\,\mathrm{d}\eta}{(\rho+\eta+1-\lambda)^2\sqrt{1-\eta^2}}, \\ \quad \frac{\lambda}{2} - (\rho + 1) \leqslant 1 \end{cases} \tag{10}$$

and

$$I_4(\rho, \lambda) = \begin{cases} \int_{-1}^{1} \frac{\rho^4\,\mathrm{d}\eta}{(\rho+\eta+1)^4\sqrt{1-\eta^2}}, \\ \quad \frac{\lambda}{2} - (\rho + 1) \geqslant 1 \\ \int_{-1}^{\lambda/2-(\rho+1)} \frac{\rho^4\,\mathrm{d}\eta}{(\rho+\eta+1)^4\sqrt{1-\eta^2}} \\ \quad + \int_{\lambda/2-(\rho+1)}^{1} \frac{\rho^4\,\mathrm{d}\eta}{(\rho+\eta+1-\lambda)^4\sqrt{1-\eta^2}}, \\ \quad \frac{\lambda}{2} - (\rho + 1) \leqslant 1 \end{cases} \tag{11}$$

respectively. The condition $\lambda/2 - (\rho + 1) \lesseqgtr 1$ arises from the definition of stress $\sigma_{\theta\theta}(x)$, see Eqs. (3) and (4). While $\lambda/2 - (\rho + 1) \leqslant 1$, the whole crack falls into the region that corresponds to $n = 0$ in expression (4). Otherwise a part of the crack (from $\lambda/2 - (\rho + 1)$ to 1) falls into the neighboring region ($n = 1$) and the expressions for the integrals (10) and (11) become more complicated.

The integrals in Eqs. (10) and (11) can be expressed in elementary functions (see [14] for details) but the results are too lengthy and not given here. Both integrals tend to zero at $\rho \to 0$ and to π at $\rho \to \infty$.

The criterion of mechanical stability of the material with crack of length l written in form (7) covers several particular cases developed earlier.

1. In the case of the classical problem of equilibrium of a crack in a uniform isotropic material loaded with uniaxial stress σ one should set both the size of stress concentrators and the normal stress at the crack surface equal to zero ($\rho = 0$ and $P_2 = 0$). The criterion of mechanical stability (7) is then reduced to

$$\frac{\sqrt{2}K}{\sqrt{l}} - \pi\sigma = 0. \tag{12}$$

The critical length l_g of the isolated crack is equal to

$$l_g = \frac{2K_g^2}{\pi\sigma_g^2}, \tag{13}$$

where $\sigma_g = \sigma$ is the applied stress and K_g is the critical stress intensity factor of a Griffith–Inglis crack in an elastic solid [13,15]

$$K_g = \sqrt{\frac{\gamma E}{\pi(1 - \nu^2)}}, \tag{14}$$

where γ is the specific energy of the crack surface, E and ν are Young's modulus and Poisson's ratio, respectively.

2. In the case of an isolated gas-filled crack in a uniform material ($\rho = 0, P_2 \neq 0$) condition (7) is reduced to

$$\frac{\sqrt{2}K}{\pi\sqrt{l}} = \sigma + P_2. \tag{15}$$

Expression (15) coincides with that obtained in [16].

3. The condition $\lambda \to \infty$ reduces the problem under consideration to that of the equilibrium of a (quasi)brittle crack formed at an isolated stress concentrator in a material subjected to uniaxial loading. The criterion of mechanical stability of the crack in this limiting case is given by

$$-\frac{\sqrt{2}K}{\sqrt{l}} + \pi(\sigma + P_2) + \left(\frac{\sigma}{2} + P_1\right)I_2(\rho) + \frac{3\sigma}{2}I_4(\rho) = 0. \tag{16}$$

The condition $\lambda \to \infty$ reduces functions $I_2(\rho)$ and $I_4(\rho)$ to the following limits:

$$\lim_{\lambda\to\infty} I_2(\rho) = I_2^\infty(\rho) = \int_{-1}^{1} \frac{\rho^2\,\mathrm{d}\eta}{(\rho + \eta + 1)^2\sqrt{1 - \eta^2}} = \pi\frac{\rho^2(\rho + 1)}{[\rho(\rho + 2)]^{3/2}} \tag{17}$$

and

$$\lim_{\lambda\to\infty} I_4(\rho) = I_4^\infty(\rho) = \int_{-1}^{1} \frac{\rho^4\,\mathrm{d}\eta}{(\rho + \eta + 1)^4\sqrt{1 - \eta^2}} = \pi\frac{\rho^4(\rho + 1)}{[\rho(\rho + 2)]^{5/2}}\,\frac{3 + 2(\rho + 1)^2}{2[\rho(\rho + 2)]}, \tag{18}$$

respectively. The corresponding problem was treated in [6].

5. The ultimate tensile strength of material with infinite row of stress concentrators

Let us rewrite condition (7) of mechanical stability in the dimensionless form:

$$-\frac{1}{\sqrt{\xi}}+\left(s+\frac{P_2}{\sigma_g}\right)+\left(\frac{s}{2}+\frac{P_1}{\sigma_g}\right)\frac{I_2(\rho,\lambda)}{\pi}+\frac{3s}{2\pi}I_4(\rho,\lambda)+\Omega_d(\rho,\lambda)\frac{\rho^2}{\lambda^2}=0, \qquad (19)$$

where $\Omega_d(\rho)$ is equal to

$$\Omega_d(\rho)=\frac{\pi}{6}\left(\pi\left(s+\frac{2P_1}{\sigma_g}\right)+2sI_2(\rho,\lambda)+3\left(\frac{2P_1}{\sigma_g}-s\right)I_4(\rho,\lambda)\right), \qquad (20)$$

where $\xi = l/l_g$ is the dimensionless crack length, and $s = \sigma/\sigma_g$ is the dimensionless external loading. The ratio of the ultimate tensile strength of material with linear row of circular stress concentrators to that of the uniform material is equal to dimensionless stress s_c corresponding to $\xi = 1$:

$$s_c=\left\{1-\left[\frac{P_2}{\sigma_g}+\frac{P_1}{\sigma_g}\frac{I_2(\rho,\lambda)}{\pi}+\frac{\pi^2}{3}\frac{P_1}{\sigma_g}\left(1+\frac{3I_4(\rho,\lambda)}{\pi}\right)\frac{\rho^2}{\lambda^2}\right]\right\}\Bigg/\left\{1+\frac{I_2(\rho,\lambda)}{2\pi}+\frac{3I_4(\rho,\lambda)}{2\pi}+\frac{\pi^2}{6}\left(1+\frac{2I_2(\rho,\lambda)}{\pi}-\frac{3I_4(\rho,\lambda)}{\pi}\right)\frac{\rho^2}{\lambda^2}\right\}. \qquad (21)$$

The stress required to initiate crack nucleation ($\rho \gg 1$) is given by the following relation:

$$s_c=\left\{1-\left[\frac{P_2+P_1}{\sigma_g}-\frac{1}{\rho}\frac{P_1}{\sigma_g}+\frac{4\pi^2}{3}\frac{P_1}{\sigma_g}\left(1-\frac{3}{\rho}\right)\frac{\rho^2}{\lambda^2}\right]\right\}\Bigg/\left\{3-\left(7-\frac{4\pi^2}{3}\frac{\rho^2}{\lambda^2}\right)\frac{1}{\rho}\right\}$$
$$\approx\frac{1}{3}\left(1-\frac{P_1+P_2}{\sigma_g}-\frac{4\pi^2}{3}\frac{P_1}{\sigma_g}\frac{\rho^2}{\lambda^2}\right)+\frac{1}{\rho}\left(\frac{7(\sigma_g-P_2)-4P_1}{9\sigma_g}+\frac{4\pi^2}{27}\frac{10P_1+P_2-\sigma_g}{\sigma_g}\frac{\rho^2}{\lambda^2}\right). \qquad (22)$$

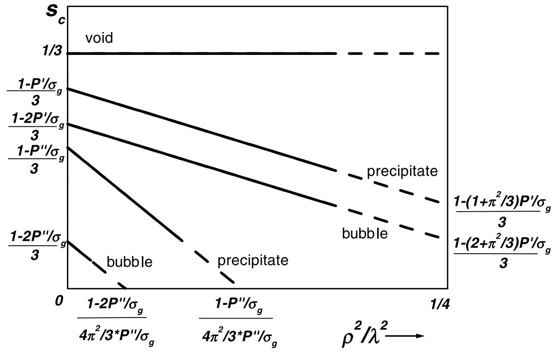

Fig. 2. Dependence of the dimensionless stress s_c required for crack formation at a stress concentrator from the row vs. ρ^2/λ^2 ratio (the terms with ρ^{-1} are neglected here). The normal stress P_1 takes on the values P' and P'', where $P'/\sigma_g < 3/(3+\pi^2)$ and $P''/\sigma_g > 3/(3+\pi^2)$ for precipitates; $P'/\sigma_g < 3/(6+\pi^2)$ and $P''/\sigma_g > 3/(6+\pi^2)$ for gas bubbles.

6. Effect of the row on the crack nucleation

It is well known (see e.g., [1–6]) that solitary stress concentrators can facilitate crack nucleation. According to Eq. (22) the row of stress concentrators increases this effect. Dependence (22) of dimensionless stress required for crack nucleation at a stress concentrator in the row is shown in Fig. 2.

It can be seen that a row of voids does not affect the nucleation of the crack. Stress required to initiate crack nucleation in this case is independent of the distance between neighboring voids and is equal to that for an isolated void ($s = 1/3$), see Fig. 2. This occurs because in the case of voids the contribution of the row to the stress tensor $\sigma_{\theta\theta}(x)$ is of the order of $(R/L)^4$ [7], i.e., beyond the accuracy adopted here. The effect of the row on the crack nucleation is weak until $L > 2R + \delta,\ \delta \ll R$ and rapidly decreases with increase of the distance between neighboring voids.

On the contrary, the row of gas bubbles ($P_1 = P_2 = P$) or precipitates ($P_1 = p > 0,\ P_2 = 0$) can noticeably reduce applied stress required to initiate crack formation. In Fig. 2 the dimensionless stress at $\rho^2/\lambda^2 = 0$ corresponds to crack nucleation at a solitary gas bubble or precipitate. Increase of the ratio ρ^2/λ^2 decreases the stress.

Normal stress P_1 acting on the row of gas bubbles or precipitates can lead to spontaneous crack nucleation provided:

$$\begin{cases}\dfrac{P_1}{\sigma_g} > \dfrac{3}{3\kappa+\pi^2}\\[2mm] \dfrac{\rho^2}{\lambda^2} > \dfrac{3(1-\kappa P_1/\sigma_g)}{4\pi^2/3P_1/\sigma_g},\end{cases} \qquad (23)$$

where $\kappa = 1$ for the case of secondary phase precipitates with normal stress $P_1 = p > 0$ acting at the precipitate–matrix interface and $\kappa = 2$ for the case of gas bubbles with internal pressure $P_1 = P$.

7. Practical applications

7.1. Voids

Nucleation and growth of ensembles of vacancy voids is a common feature of structural materials under irradiation. It is known that degradation of service properties of these materials takes place due to formation of voids.

Let us evaluate the ultimate tensile strength of uniaxially loaded material with infinite row of circular voids. There is no normal stress at the surface of void and crack, i.e., $P_1 = P_2 = 0$. According to Eq. (21) the ultimate tensile strength in this case is

$$s_c = \left\{ 1 + \frac{I_2(\rho,\lambda)}{2\pi} + \frac{3I_4(\rho,\lambda)}{2\pi} + \frac{\pi^2}{6}\left(1 + \frac{2I_2(\rho,\lambda)}{\pi} - \frac{3I_4(\rho,\lambda)}{\pi}\right)\frac{\rho^2}{\lambda^2} \right\}. \quad (24)$$

Dependence of $s_c(\rho,\lambda)$ is shown in Fig. 3. Several typical cross-sections of the surface $s_c(\rho,\lambda)$ are given in Fig. 4. Curves 4 and 5 in Fig. 4 correspond to large distances between the neighboring voids ($\lambda \gg 1$). In this case the row represents dilute ensemble of voids and the problem of crack nucleation and growth can be treated within the approach developed in [6]. Reduction of the distance between neighboring voids increases the influence of the row on the crack evolution and facilitates crack growth in comparison with that of the crack formed at an isolated void. As a result the ultimate tensile strength of the material is decreased (see curves 1–3 in Fig. 4). In the case when the distance between surfaces of neighboring voids tends to zero one should be careful because in this case the adequate evaluation of the ultimate tensile strength of the material requires the account of additional terms in expansion of $\sigma_{\theta\theta}(x)$ (see Eq. (3)) into series over $(R/L)^2$.

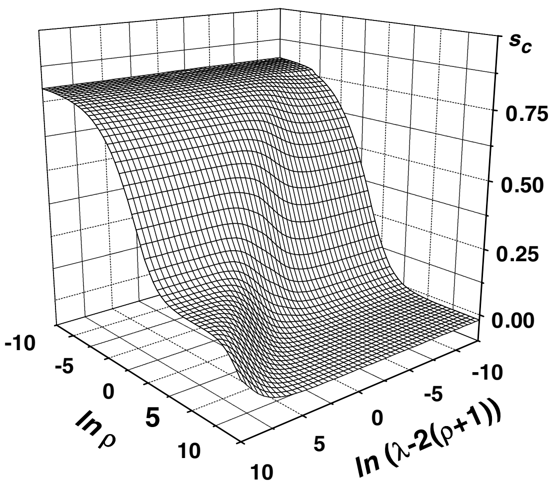

Fig. 3. Dependence of the ultimate tensile strength $s_c(\rho,\lambda)$ of uniaxially loaded material with row of voids.

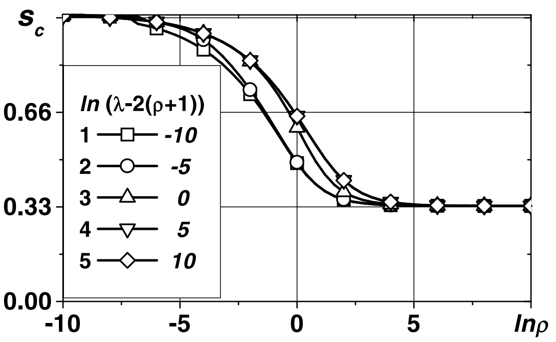

Fig. 4. Typical cross-sections of the surface $s_c(\rho,\lambda)$ shown in Fig. 3.

7.2. Gas bubbles

Irradiation of a material with fast particles can result not only in its supersaturation with point defects, but may sometimes produce non-equilibrium concentration of gas (e.g., helium) atoms due to transmutation nuclear reactions and/or direct α-particles implantation. Supersaturated multi-component solid solution of gas atoms, self-interstitials and vacancies decays with gas bubble ensemble nucleation and evolution [17]. It is generally accepted that high temperature irradiation embrittlement arises because of helium bubble ensemble formation.

Let us evaluate the ultimate tensile strength of strained material with an infinite row of gas bubbles. Because of the presence of gas, internal surfaces of bubbles and the crack are loaded with normal stress $P_1 = P_2 = P$. The normalized ultimate tensile strength s_c in this case is given by the following relation:

$$s_c = \left\{ 1 - \frac{P}{\sigma_g}\left[1 + \frac{I_2(\rho,\lambda)}{\pi} + \frac{\pi^2}{3}\left(1 + \frac{3I_4(\rho,\lambda)}{\pi}\right)\frac{\rho^2}{\lambda^2}\right] \right\} \Big/ \left\{ 1 + \frac{I_2(\rho,\lambda)}{2\pi} + \frac{3I_4(\rho,\lambda)}{2\pi} + \frac{\pi^2}{6}\left(1 + \frac{2I_2(\rho,\lambda)}{\pi} - \frac{3I_4(\rho,\lambda)}{\pi}\right)\frac{\rho^2}{\lambda^2} \right\}. \quad (25)$$

Dependence (25) of the ultimate strength $s_c(\rho,\lambda)$ is shown in Fig. 5. It was found [6] that the volume of formed crack can be neglected in comparison with that of the bubble for all application relevant cases. So, the internal pressure can be assumed invariable during the crack formation and growth.

Several typical cross-sections of the surface $s_c(\rho,\lambda)$ are given in Fig. 6. Curve 5 corresponds to the case of large inter-bubble distance ($\lambda \gg 1$). Effect of the row becomes apparent for very large gas bubbles only ($\rho \gg 1$). For relatively small gas bubbles the influence of the neighborhood can be neglected and the problem can

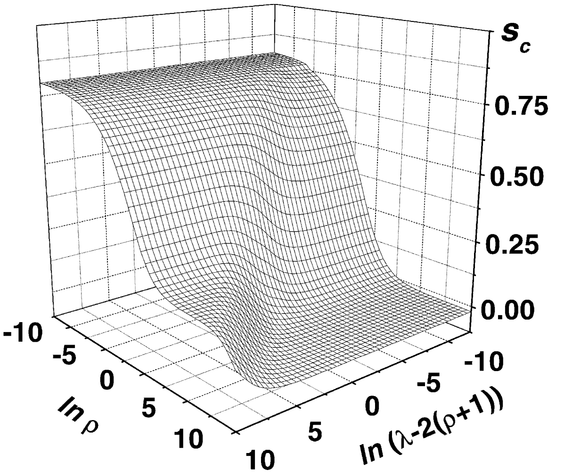

Fig. 5. Dependence of the ultimate strength $s_c(\rho, \lambda)$ of uniaxially loaded material with row of gas bubbles. Internal gas pressure $P = 0.2\sigma_g$.

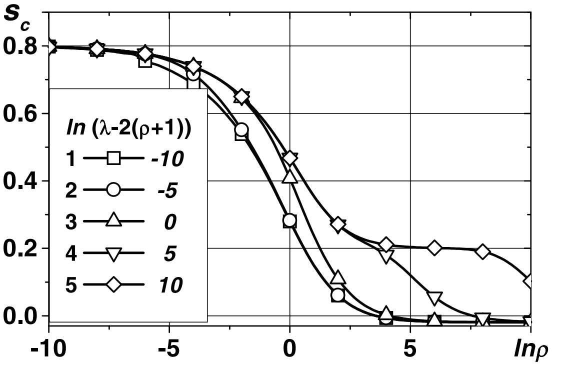

Fig. 6. Typical cross-sections of the surface $s_c(\rho, \lambda)$ shown in Fig. 5.

be treated in the assumption of a solitary bubble [6]. Reduction of the distance between centers of neighboring bubbles results in increase of the row effect (curves 1–4 in Fig. 6). At large ρ^2/λ^2 ratio spontaneous nucleation of crack at a bubble in the row can occur (the ultimate tensile strength falls to zero value, see downward excursion of the surface $s_c(\rho, \lambda)$ in Fig. 5 and curves 1–4 in Fig. 6). In the opposite case of very small gas bubbles ($\rho \to 0$) the effect of the row on the crack evolution is weak and we can neglect both the row and the bubble influence. The problem reduces to that of gas filled crack in the uniform material [16]. This is the only case when the volume of the crack cannot be neglected.

7.3. Secondary phase precipitate

In order to improve service properties, materials are often doped and subjected to thermal treatment. Mentioned material processing techniques can result in secondary phase precipitation. High environment temperature and fast particle irradiation can also activate diffusion redistribution of material components and lead to formation of secondary phase precipitates. Very often spatial distribution of precipitates is not uniform. They can form ordered ensembles at grain boundaries, triple grain junctions, etc. In general the effect of precipitation can be both positive and negative [6].

7.3.1. Effect of precipitation on crack nucleation

Normal stress $P_1 = p$ acting at the precipitate–matrix interface influences significantly the nucleation of wedge crack at a precipitate from the row. Dependence of the crack nucleation load on ρ^2/λ^2 ratio is shown in Fig. 7. The dependence is drawn for several values of normal stress p at the precipitate–matrix interface. It is clear that when $p \geqslant 0$ the crack nucleation at a precipitate in the row is facilitated, i.e., the situation is similar to crack nucleation at the row of gas bubbles or voids, see Fig. 2. However, in contrast to bubbles and voids, secondary phase precipitates can create tensile stress (negative within current consideration) in the surrounding matrix. In this case the effect of the row becomes more complicated, see Fig. 7. Facilitated nucleation of crack at a precipitate from the row occurs provided

$$\begin{cases} \dfrac{p}{\sigma_g} < \dfrac{6}{3+\pi^2} \approx 0.47 \\ \dfrac{\rho^2}{\lambda^2} < \dfrac{2 - p/\sigma_g}{4\pi^2/3p/\sigma_g}, \end{cases} \tag{26}$$

is satisfied. (Here the absolute value of tensile stress p is implied.)

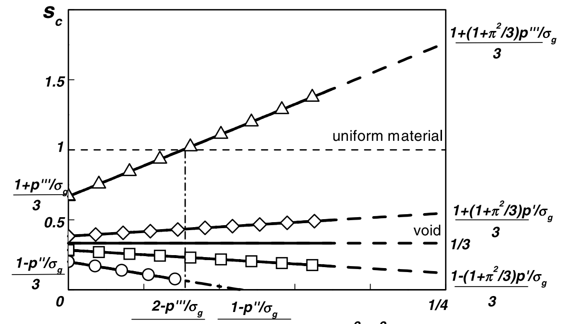

Fig. 7. Dependence of the dimensionless stress s_c required for crack formation at a precipitate in the row vs. ρ^2/λ^2 ratio at different actual stress at tte precipitate–matrix interface. Here the normal stress P_1 takes on the following values: $P_1 = p''$ (○), $p''/\sigma_g > 3/(3+\pi^2)$; $P_1 = p'$ (□), where $p'/\sigma_g < 3/(3+\pi^2)$; $P_1 = -p'$ (◇) tensile stress at the precipitate–matrix interface; $P_1 = -p'''$ (△), where $p'''/\sigma_g \geqslant 6/(3+\pi^2)$.

7.3.2. The ultimate tensile strength of material with precipitates

Below we evaluate the ultimate tensile strength of a material with an infinite row of secondary phase precipitate. Normal stress is acting at the precipitate–matrix interface: $P_1 = p$, while normal stress acting at the crack surface is absent ($P_2 = 0$). The normalized ultimate tensile strength is given by the following relation:

$$s_c = \left\{1 - \frac{p}{\sigma_g}\left[\frac{I_2(\rho,\lambda)}{\pi} + \frac{\pi^2}{3}\left(1 + \frac{3I_4(\rho,\lambda)}{\pi}\right)\frac{\rho^2}{\lambda^2}\right]\right\} \Big/ \left\{1 + \frac{I_2(\rho,\lambda)}{2\pi} + \frac{3I_4(\rho,\lambda)}{2\pi} + \frac{\pi^2}{6}\left(1 + \frac{2I_2(\rho,\lambda)}{\pi} - \frac{3I_4(\rho,\lambda)}{\pi}\right)\frac{\rho^2}{\lambda^2}\right\}. \quad (27)$$

Modification of strength properties by secondary phase precipitates depends on the local stress field around the precipitate. Presence of the row of precipitates results in reduction of the ultimate tensile strength provided normal stress at the precipitate–matrix interface is directed out of a precipitate ($p > 0$), i.e., precipitates 'compress' surrounding matrix. Tensile stress ($p < 0$) at the precipitate–matrix interface can either decrease or increase the ultimate tensile strength of the local region containing precipitates.

Reduction of the ultimate strength $s_c(\rho, \lambda)$ due to presence of the row of precipitates with positive normal stress $P_1 = p > 0$ is similar to that for the row of gas bubbles (see Fig. 5 and Eq. (6)). The main difference is in zero magnitude of the normal stress P_2 in the case of precipitates that affects the actual value of the ultimate tensile stress but does not change the general behavior.

Dependence of the ultimate strength on tensile stress produced by the row of precipitates in the surrounding matrix is more complicated. It was shown above that it can suppress nucleation of the crack at a precipitate in the row. The ultimate tensile strength of the material vs. normal stress p and the distance between neighboring precipitates is shown in Fig. 8. Several surfaces $s_c(\rho, \lambda)$ with different values of normal stress $P_1 = p$ are built up. Dependence Fig. 8(a) and corresponding typical cross-sections Fig. 8(b) are built up for normal stress $p = -0.2\sigma_g$. The shape of the surface $s_c(\rho, \lambda)$ significantly changes in comparison with that for normal stress $p = 0.2\sigma_g$ (see Figs. 5 and 6). For large distances between neighboring bubbles ($\lambda \gg 1$) the qualitative behavior in the cases $p = 0.2\sigma_g$ and $p = -0.2\sigma_g$ looks similar, i.e., facilitated [1] nucleation of crack at the precipitate surface occurs and the effect of the row of precipitates falls with crack length increase (when $\rho \to 0$). However, the absolute value of applied stress resulting in crack formation is higher in the case of tensile stress $p = -0.2\sigma_g$ in comparison with that for $p = 0.2\sigma_g$. The principal difference occurs with the decrease of the distance between the precipitates. In the case of 'positive' stress at the precipitate surface the spontaneous crack nucleation can occur, see Figs. 5 and 6. In the case of tensile normal stress at a precipitate surface the spontaneous nucleation is impossible.

Further increase of the actual tensile stress at the precipitate–matrix interface up to $p = -\sigma_g$ results in additional modification of the surface $s_c(\rho, \lambda)$, see Fig. 8(c) and (d). Curve with diamonds in Fig. 8(d) corresponds to large distance between precipitates. Nucleation of crack in this case is impeded by tensile stress field in the surrounding matrix, see Eq. (26). If a precipitate radius is not large, the presence of the row of precipitates results in reduction of the ultimate tensile strength, see curve with down triangles and up triangles in Fig. 8(d). However decrease of the distance between precipitates leads to reduction of ρ values region where s_c is less than 1. Nucleation of crack on a precipitate is prohibited by stress field formed around the row. Decrease of the distance between precipitates (curves with circles and squares in Fig. 8(d)) leads to effect of local strengthening of the material region containing the row of precipitates. In this case the ultimate tensile strength in the vicinity of the row of precipitates is higher than that for the uniform material.

Figs. 8(e) and (f) illustrate the case of the tensile stress $p = -2\sigma_g$ at the precipitate–matrix interface when nucleation and evolution of crack are suppressed for any ρ and λ values.

8. Summary

The problem of crack formation at a linear array of stress concentrators is considered. In terms of the force balance approach a general equation for the crack length as a function of external and internal parameters is obtained. In the case of a critical crack this equation can be used for evaluation of the ultimate tensile strength of material with a linear row of stress concentrators.

The ultimate tensile strength of material with the row of voids, gas bubbles or secondary phase precipitates is found. The relative degradation of strength properties as a function of size of stress concentrators in the row, the distance between neighboring stress concentrators and the normal stress acting at a stress concentrator surface is established. It is shown that the presence of the row of voids and gas bubbles facilitates crack nucleation and growth in comparison with the case of crack formation at a solitary gas bubble or void. Favored crack nucleation and evolution also occurs in the case of the row of secondary phase precipitates provided the normal stress

[1] In comparison with the uniform material.

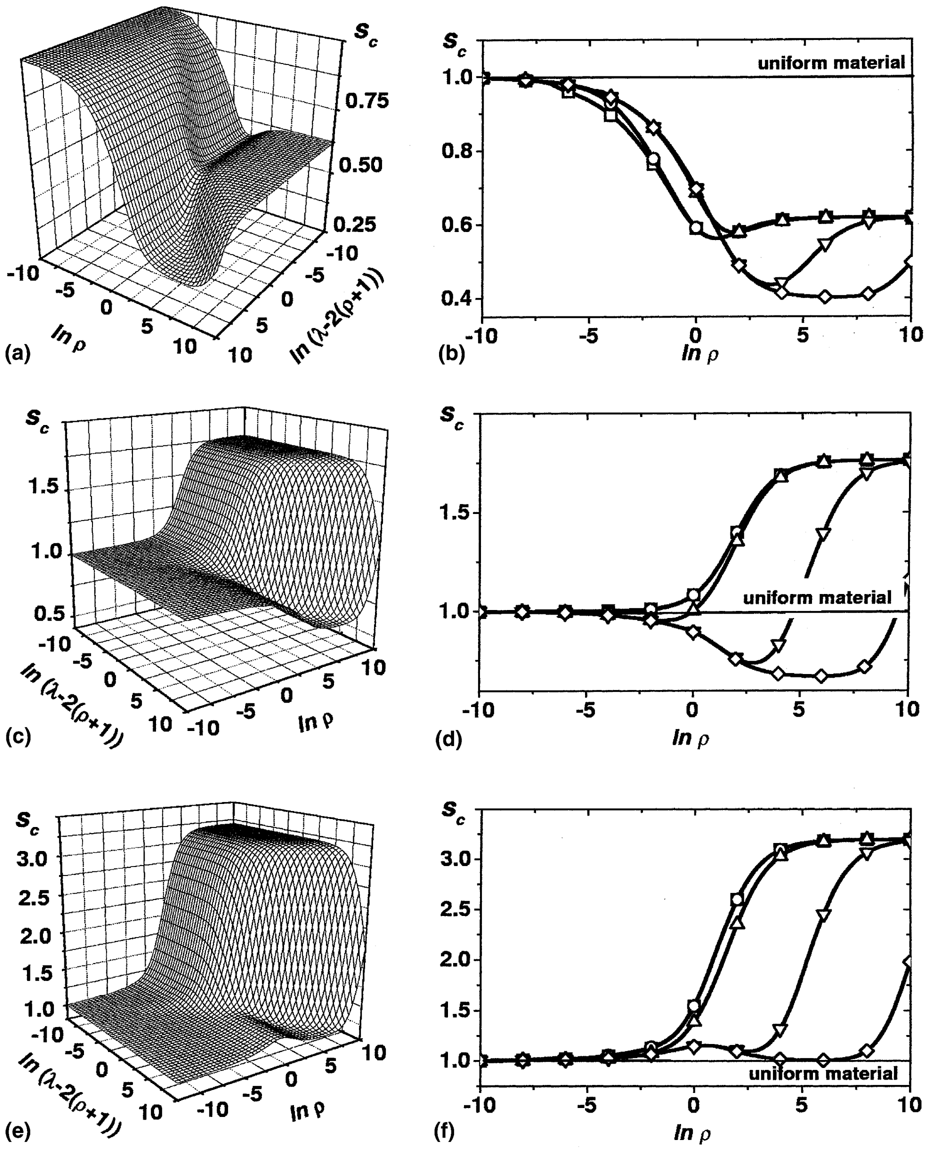

Ln(λ-2(ρ+1))	10	5	0	-5	-10
symbol	◇	▽	△	○	□

Fig. 8. Modification of the surface $s_c(\rho, \lambda)$ with increase of tensile stress p at the precipitate–matrix interface. Figures (a), (c), (e) represent dependence $s_c(\rho, \lambda)$ at $p = -0.2\sigma_g$, $p = -\sigma_g$ and $p = -2\sigma_g$, respectively. Corresponding typical cross-sections are shown in figures (b), (d) and (f).

at the precipitate–matrix interface is directed out of precipitates. Spontaneous crack nucleation is possible if either the pressure (for gas bubbles) or the normal stress (for precipitates) is high enough: $P/\sigma_g \geqslant 3/(6+\pi^2) \approx 0.19$ for gas bubbles; $p/\sigma_g \geqslant 3/(3+\pi^2) \approx 0.23$ for precipitates and the distance between the neighboring stress concentrators is relatively small (see Eq. (23) for details). The corresponding values are $P/\sigma_g \geqslant 0.5$ for a solitary gas bubble and $P/\sigma_g \geqslant 1$ for solitary precipitate.

More complicated dependence of crack nucleation and growth takes place for precipitates that generate tensile stress field in the surrounding matrix. Spontaneous crack nucleation is impossible in this case. Facilitated crack nucleation and growth of crack at the precipitate in the row occurs provided $p/\sigma_g \leqslant 6/(3+\pi^2) \approx 0.46$ ($p/\sigma_g \leqslant 2$ for the solitary precipitate). The effect of the row can vary from positive (impeded crack nucleation) to negative (facilitated crack growth) during crack evolution provided $6/(3+\pi^2) \leqslant p/\sigma_g \leqslant 2$.

References

[1] Y. Murakami, in: Stress Intensity Factors Handbook, vol. 1, Pergamon, Oxford, 1987, p. 241.
[2] J.C. Newman, NASA TN D-6376 (1971) 1.
[3] J. Tweed, D.P. Roohe, J. Eng. Sci. 11 (1973) 1185.
[4] J. Schijve, Int. J. Fracture 23 (1983) r111.
[5] O.L. Bowie, J. Math. Phys. XXXV (1) (1956) 60.
[6] R.E. Voskoboinikov, J. Nucl. Mater. 270 (1999) 309.
[7] V.A. Borodin, V.M. Manichev, A.I. Ryazanov, J. Nucl. Mater. 189 (1992) 124.
[8] H. Schroeder, W. Kesternich, H. Ullmaier, Nucl. Eng. Des./Fusion 2 (1985) 65.
[9] H. Schroeder, D.N. Braski, J. Nucl. Mater. 115 (1983) 297.
[10] H. Liebovitz (Ed.), Fracture. An Advanced Treatise, vol. II, Academic, New York, 1968.
[11] R.E. Voskoboinikov, J. Nucl. Mater. 280 (2000) 169.
[12] L.D. Landau, E.M. Livshits, Theory of Elasticity, Pergamon, Oxford, 1969.
[13] Yu.P. Raizer, Sov. Phys. Docl. 13 (1970) 129.
[14] A.P. Prudnikov, Yu.A. Brichkov, O.I. Marichev, Integrals and Series. Elementary Functions, Nauka, Moscow, 1981 (in Russian).
[15] J. Weertman, Dislocation Based Fracture Mechanics, World Scientific, Singapore, 1996.
[16] V.A. Borodin, V.M. Manichev, A.I. Ryazanov, Sov. Phys. Solid State 36 (1990) 331.
[17] R.E. Voskoboinikov, A.E. Volkov, J. Nucl. Mater. 282 (2000) 66.